Bull. Mater. Sci., Vol. 38, No. 4, August 2015, pp. 1055–1059. © Indian Academy of Sciences.

Study of influence on micro-fabricated resistive switching organic ZrO_2 array by C-AFM measurement

YING LI[1,*], GAOYANG ZHAO[2], ZHIBO KOU[3], LONG JIN[2] and YAJING WANG[2]

[1]Advanced Material Analysis Center, Xi'an University of Technology, Xi'an, Shaanxi 710048, China
[2]Material Science and Engineering School, Xi'an University of Technology, Xi'an, Shaanxi 710048, China
[3]Northwest Electric Power Design Institute of China Power Engineering Consulting Group, Xi'an, Shaanxi 710075, China

MS received 18 September 2014; accepted 5 February 2015

Abstract. **In this paper, a comparison of the interfacial electronic properties between Pt/Ir conductive atomic force microscopy (C-AFM) tip and ZrO_2 organic array was carried out. A uniformed ZrO_2 array was fabricated with a mean diameter of around 1 μm using laser interference lithography. A C-AFM measurement set-up was built up. The *I–V* curve was directly measured of the organic ZrO_2 array which shows a resistive switching characteristic by C-AFM measurement. The set voltage is 18.0 V and the reset voltage is −5.0 V. After the Pt layer was coated on the ZrO_2 array, the set voltage decreases to 0.8 V and the reset voltage decreases to −2.2 V. This result shows that Pt layer can prevent the potential drop effectively. The electron barrier height between Pt/Ir C-AFM tip and organic ZrO_2 array was enhanced by sputtering Pt layer on the ZrO_2 organic array.**

Keywords. **Surface measurement; ZrO_2 array; C-AFM; resistive switching.**

1. Introduction

The study of organic-based devices, like transistors and light-emitting diodes (FETs, OLEDs), is developed very fast over the last decade.[1] At the same time resistive switches have been observed on organic and polymer films.[2] This study gives rise to an important application of organic thin film devices as memory devices. For the next-generation non-volatile memory material, the most promising candidate is resistive random access memory (RRAM) which is non-volatile memories with high-density, high-speed and low-power consumption.[3–5]

For further applications, it is still a challenge to fabricate nano-structures of RRAM material. Micro-fabrication methods involve traditional lithography, chemical etching, electron beam directly writing, nano-imprint and so on. However, the procedure and the cost of these methods are relatively complicated and expensive for semiconductors process. In this paper, we demonstrate a promising and low-cost method for fabricating sub-micro-ZrO_2 lattice by using the sol–gel method combined with laser interference lithography.

Despite the extensive research, much of the underlying mechanism is still unclear and controversial. This task could be accomplished only with advanced measurement and technique such as *in situ* high-resolution transmittance electron microscopy (HRTEM), conductive atomic force microscopy (C-AFM) and so on.[6–8] In this paper, the interfacial electronic properties between organic ZrO_2 array and C-AFM tip have been investigated. In our research, the RRAM unit consists of a C-AFM tip as an anode, a ZrO_2 array dot as RRAM material and a Cu electrode as a cathode. A uniform ZrO_2 array dot with a mean diameter of about 1 μm is fabricated by the photosensitive sol–gel method combined with laser interference lithography. Hence, we can directly measure the *I–V* curves of the ZrO_2 lattice dot with the C-AFM tip. In this method, we can avoid the influence from read-to-read crosstalk and influence from micro-fabricate process.

2. Experimental

2.1 *ZrO_2 lattice preparation*

Photosensitive ZrO_2 films were fabricated with the metal alkoxide zirconium tetra-n-butoxide [$Zr(OC_4H_9)_4$], benzoylacetone (BzAcH) and ethanol (EtOH) in the molar ratio of Zr : BzAcH : EtOH at 1 : 1 : 40. After mixed and refluxed for 2–3 h, the photosensitive ZrO_2 solution was obtained. Then using the dip coating method ZrO_2 organic films were formed on Cu substrate. The Cu substrates were fabricated by magnetic sputtering. The UV–visible absorption spectra was measured which is shown in figure 1. These spectra of the ZrO_2 films were dip-coated on quartz glass substrate. It was known that an absorption peak of BzAcH at 308 nm due to the π-to-π^* transition. These peaks shift to 338 nm in the spectra of the ZrO_2 gel films. This red shift indicates the chelation between Zr^{4+} and BzAcH, and the reaction results in the partial replacement of the alkoxy group by β-diketone

*Author for correspondence (liying@xaut.edu.cn)

ligand (see equation (1)). Figure 1 also shows the change of optical absorption spectra of ZrO_2 films irradiated by a UV Kr ion laser. The intensity of absorption peaks at around 338 nm decreases step by step with increasing irradiation time from 0 to 400 s. These decreasing spectra showed that the chelate rings were dissociated by UV irradiation.

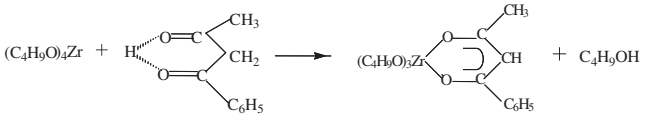

(1)

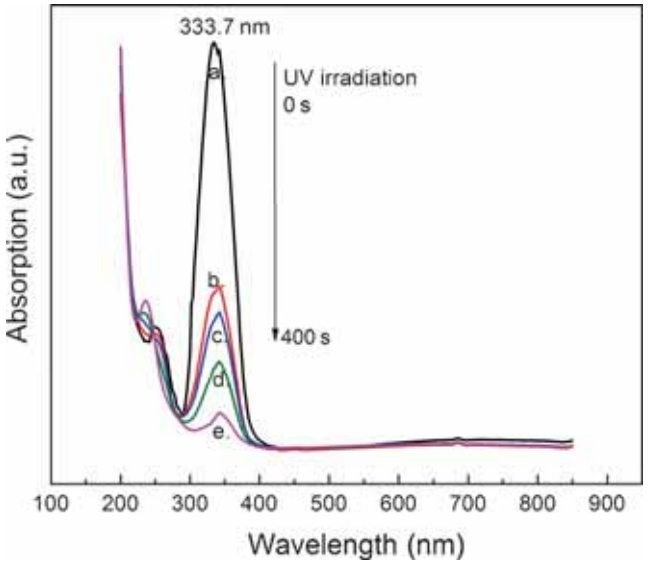

Figure 1. The UV–visible absorption spectra of the photosensitive ZrO_2 film.

ZrO_2 array were fabricated by double exposures of two-beam laser interference through 90° degrees rotating the sample in its own plane between twice exposures with 350 nm Krypton ion laser. After laser exposure, the exposed part of ZrO_2 gel film is not soluble in leaching solution while the unexposed part is still soluble. Therefore, organic ZrO_2 array can be obtained.[9,10]

2.2 *Local C-AFM measurement systems*

This C-AFM measurement system is consisted with an AFM (Seiko Instruments Inc., SPI3800N/SPA-400) with a resolution of 0.1 nm in the x–y directions and 0.01 nm in the z direction and a Keithly 2400 I–V source meter (Keithly, USA). The conductive tips (PPP-CONT, Nanosensors) were coated by sputtering deposition with a 25-nm-thick double layer of chromium and Pt/Ir with an initial 20 nm radius. In our C-AFM measurement study, RRAM unit consists of a C-AFM tip as an anode, a ZrO_2 array dot as RRAM material and a Cu electrode as a cathode. The current–voltage (I–V) curves were measured in air at room temperature as shown in figure 2. In order to identify the RRAM properties of ZrO_2 array, the Pt/Ir C-AFM tip is positioned at the centre of one of the dots. During the C-AFM measurement, Pt/Ir conductive probe and the base of the C-AFM are connected to Keithly 2400 meter to apply the excitation signal and record voltage and current response of the RRAM array dots. When the voltages from Keithly 2400 meter are applied to the Pt/Ir C-AFM tip and Cu bottom electrode of the sample, the current flow occurs through the cantilever and goes back to the Keithly 2400 meter. Then a local I–V curve can be obtained.

In order to solve the influence from huge contact resistance between the Pt/Ir C-AFM tip and a single ZrO_2 array, a Pt layer was covered on the whole ZrO_2 lattice by sputtering.

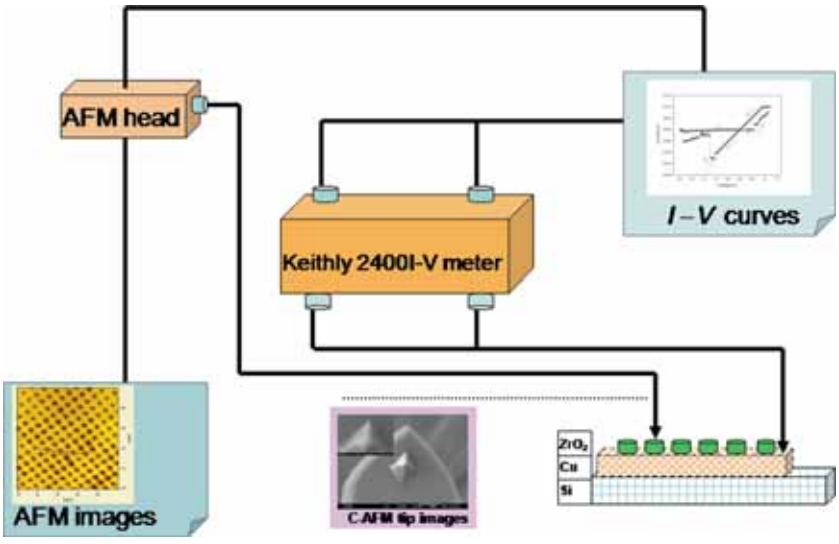

Figure 2. Diagram of C-AFM set-up equipment.

3. Discussion and results

3.1 *Local I–V curves by C-AFM measurement systems*

During the C-AFM measurement, the parameters of I Gain and P Gain should be adjusted. The value of P Gain should be set as 1/3 of I Gain value. The Pt/Ir conductive coating could be off when the value of Force Reference (For. Ref.) is too small. This value should be set from -1 to -4 nm. The sweep voltage can be set from -25 to 25 V. Figure 3a and b shows the local C-AFM images of ZrO_2 array 2D and 3D, respectively. The measured area is 10×10 μm. The profile image is shown in figure 3c. The height of array dot A (ΔZ) is about 61 nm and dot B (ΔZ) is about 58 nm. The distance shown in figure 3c is the half of diameter. The diameter of dot A is about 1.2 μm and dot B is about 1.1 μm. Figure 3d and e shows local I–V curves which are measured while the C-AFM image was scanning. The current compliance (CC) is applied to 100 μA during I–V sweep. When the voltage goes to 18.0 V, the current increases rapidly which means the OFF state switches to the ON state. During the negative side I–V sweep, when the voltage goes to -5.0 V, the current decreases rapidly which means the ON state switches to the OFF state. In order to make sure the array dot is not shift during the C-AFM measurement, an AFM image scan is very necessary after the local I–V

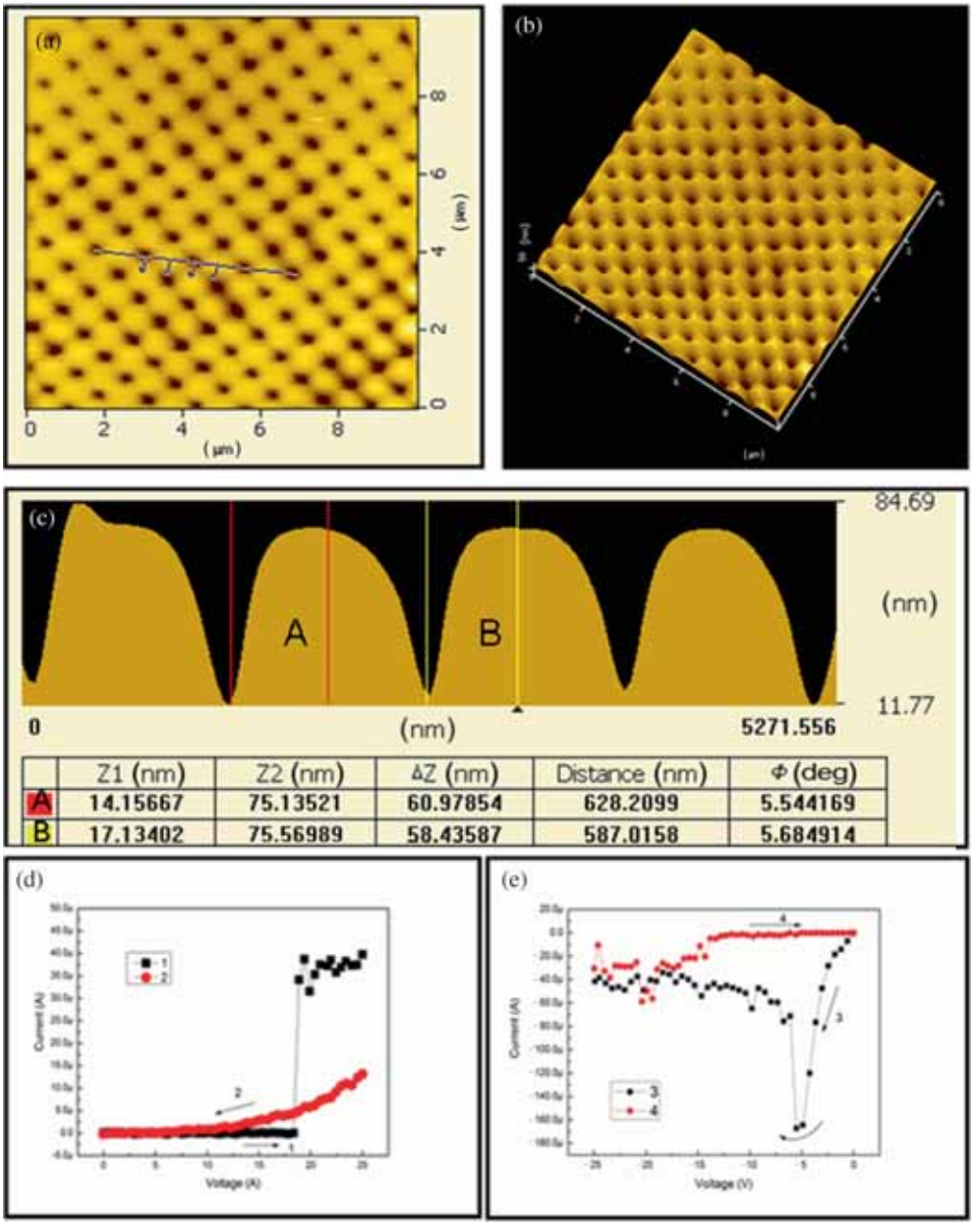

Figure 3. Local observation of ZrO_2 lattice dot by C-AFM measurement systems. (**a**) Two dimensions and (**b**) three dimensions images of the ZrO_2 lattice dot. (**c**) Profile image of the ZrO_2 lattice dot. (**d**) Local I–V curves measured at positive voltage and (**e**) negative voltage.

measurement finished. It gives off a large amount of Joule heat when the current is moving through the filaments. This result shows that the required switching voltage to set into low resistance state under C-AFM set-up is larger than on normal Cu/ZrO_2/ATO cell. It is attributed to the formation of an adsorbate film between Pt/Ir conductive tip and the ZrO_2 array dot. This could cause an additional potential drop.[11,12]

3.2 *Influence on a Pt layer by C-AFM measurement systems*

Influence from the micro-fabricate process was shown clearly which the set and reset voltage increased compared with the normal ZrO_2 thin films.[13] In order to decrease the contact resistance from the formation of an adsorbate film between Pt/Ir conductive tip and the ZrO_2 array dot, a Pt layer was covered on the whole ZrO_2 array by sputtering.

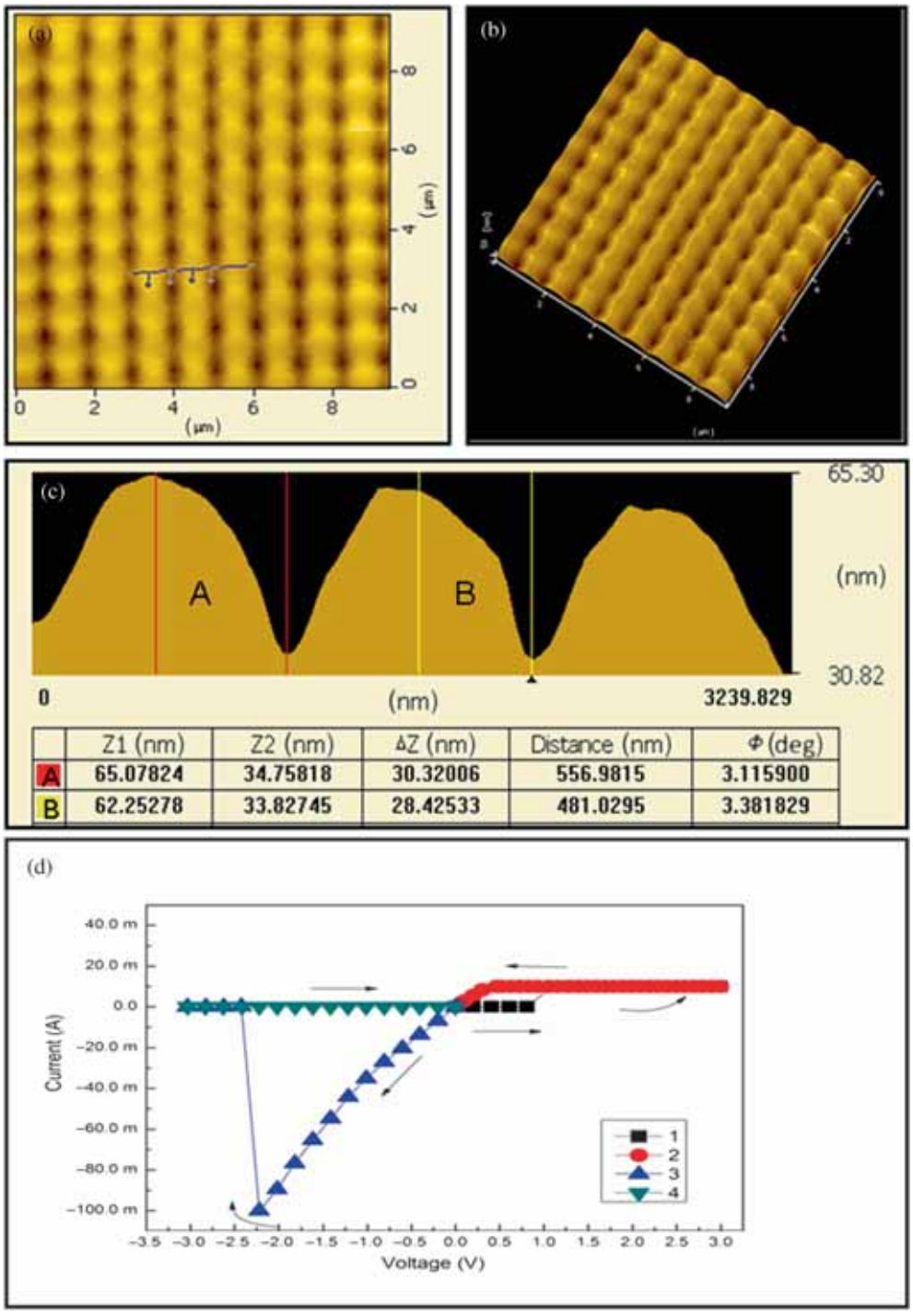

	Z1 (nm)	Z2 (nm)	ΔZ (nm)	Distance (nm)	Φ (deg)
A	65.07824	34.75818	30.32006	556.9815	3.115900
B	62.25278	33.82745	28.42533	481.0295	3.381829

Figure 4. Local observation of ZrO_2 lattice dot which is covered by the sputtered Pt by C-AFM measurement systems.

Figure 4a and b shows the C-AFM images of ZrO_2 array 2D and 3D after a Pt film sputtered on ZrO_2 lattice. The measured area is 10 $\times$10 μm. The profile image is shown in figure 4c. The height of array dot A (ΔZ) is about 30 nm and dot B (ΔZ) is about 28 nm. The diameter of dot A is about 1.1 μm and dot B is about 0.8 μm. The height of array dot decreased about 30 nm for the sputtering of Pt film on ZrO_2 lattice dot. Figure 4d is a local I–V curve which is also measured while the C-AFM image was scanning. The current compliance (CC) is applied to 100 μA during I–V sweep. When the voltage goes to 0.8 V, the current increases rapidly which means the OFF state switches to the ON state. During the negative side I–V sweep, when the voltage goes to −2.2 V, the current decreases rapidly which means the ON state switches to the OFF state. This result shows that Pt layer can prevent the potential drop effectively.

Work functions of Cu and Pt/Ir are 4.65 and 5.50 eV, respectively.[14] When a Pt layer was sputtering on ZrO_2 array it is proved that the set voltage decreases from 18.0 to 0.8 V while the reset voltage also decreases from −5.0 to −2.2 V, which are relative to the electron injection from the Pt/Ir C-AFM tip to ZrO_2 organic array. The electron barrier height between Pt/Ir C-AFM tip and ZrO_2 organic array is enhanced by using Pt layer sputtered. The electron barrier height between Pt/Ir C-AFM tip and ZrO_2 organic array was enhanced by sputtering Pt layer on the ZrO_2 organic array.

4. Conclusion

A uniformed ZrO_2 array with a mean diameter of around 1 μm is formed using laser interference lithography. A C-AFM measurement set-up was built. Futher the I–V curves of the ZrO_2 array were directly measured. The set voltage is 18.0 V and the reset voltage is −5.0 V. When the Pt layer was coated on the ZrO_2 array, the set voltage decreased to 0.8 V and the reset voltage decreased to −2.2 V. The contact resistance decreased after a Pt film sputtered on ZrO_2 array. Joule heat moving through the filaments also goes down. This is a effective way to protect the micro-fabricated resistive switching unit. And also the electron barrier height between Pt/Ir C-AFM tip and ZrO_2 organic array was enhanced by sputtering Pt layer on the ZrO_2 organic array. Low resistive switching voltage fine fabricated ZrO_2 organic arrays were fabricated.

Acknowledgements

This work was supported by the National Natural Science Foundation of China (No. 51372198). We thank the Foundation of young teachers of Xian University of Technology. We also thank the National Natural Science Foundation of China (No. 51202190).

References

1. Horowitz G 1998 *Adv. Mater.* **10** 365
2. Oyamada T, Tanaka H, Matsushige K, Sasabe H and Adachi C 2003 *Appl. Phys. Lett.* **83** 1252
3. Biju K P, Liu X, Kim J, Jung S, Lee J and Hwang H 2011 *Curr. Appl. Phys.* **11** S102
4. Li Y and Long S 2010 *IEEE Electron. Device Lett.* **31** 117
5. Peng S, Fei Z, Chen X, Zhu X and Li R 2011 *Appl. Phys. Lett.* **100** 072101
6. Tiedke S and Schmitz T 2001 *Appl. Phys. Lett.* **79** 3678
7. Wojtyniak M, Szot K and Waser R 2011 *Appl. Surf. Sci.* **257** 7627
8. Yang L, Kuegeler C, Szot K, Ruediger A and Waser R 2009 *Appl. Phys. Lett.* **95** 013109
9. Wang Z and Zhao G 2008 *Sci. China Ser. E-Technol. Sci.* **51** 1995
10. Wang Z and Zhao G 2011 *J. Non-Cryst. Solids* **357** 1223
11. Peter F, Szot K, Waser R, Reichenberg B, Tiedke S and Szade J 2004 *Appl. Phys. Lett.* **85** 2896
12. Peter F, Kubacki J, Szot K, Reichenberg B and Waser R 2006 *Phys. Status Solidi A* **203** 616
13. Awais M N, Muhammad N M, Navaneethan D, Kim H C, Jo J and Choi K H 2013 *Microelectron. Eng.* **103** 167
14. Su W S, Chena Y F, Hsiao C L and Tu L W 2007 *Appl. Phys. Lett.* **90** 063110